2009 American Control Conference
Hyatt Regency Riverfront, St. Louis, MO, USA
June 10-12, 2009

Underwater Mine Detection using Symbolic Pattern Analysis of Sidescan Sonar Images★

Chinmay Rao crr164@psu.edu
Kushal Mukherjee kum162@psu.edu
Shalabh Gupta szg107@psu.edu
Asok Ray axr2@psu.edu
Shashi Phoha sxp26@psu.edu
The Pennsylvania State University
University Park, PA 16802

Abstract— **This paper presents symbolic pattern analysis of sidescan sonar images for detection of mines and mine-like objects in the underwater environment. For robust feature extraction, sonar images are symbolized by partitioning the data sets based on the information generated from the ground truth. A binary classifier is constructed for identification of detected objects into mine-like and non-mine-like categories. The pattern analysis algorithm has been tested on sonar data sets in the form of images, which were provided by the Naval Surface Warfare Center. The algorithm is designed for real-time execution on limited-memory commercial-of-the-shelf platforms, and is capable of detecting seabed-bottom objects and vehicle-induced image artifacts.**

Index Terms— **Symbolic Dynamics, Pattern Recognition, Mine Countermeasures**

I. Introduction

Rapid advancement of modern engineering technology has led to development of increasingly portable manned and unmanned platforms for mine countermeasure (MCM) operations. In particular, unmanned undersea vehicles (UUV) provide enhanced speed and improved search efficiency in MCM operations. These vehicles are equipped with advanced sensing devices, including sidescan sonar imaging systems, to search a target area for detection of mines and mine-like objects in the underwater environment. However, this paper makes no distinction between mines and mine-like objects because they are both represented by the same features in the sonar image; hence, both mines and mine-like objects are simply referred to as mines in the sequel. Once a mine is detected, more precise measurement (possibly using other sensors) and analysis is required to distinguish between mines and mine-like objects that might have been falsely identified as mines. The latter task is a topic of future research and is not addressed in this paper.

The current state-of-the-art MCM techniques involve deployment of assets that perform sequential operations of detection, classification, and neutralization [6]. For MCM operations, side-scan sonar systems are typically used for efficient imaging of large areas of the sea floor. These devices generate a monochromatic mapping of seabed-bottom objects and vehicle-induced image artifacts.

The traditional approach to mine detection problem is to simply assign a threshold to the mapped features, based on the premise that the object should be brighter (i.e., have a stronger reflected signal) than the background of a sonar image. This approach works well for a relatively featureless background; however, a textured background may encounter many false positive mine locations. Recent mine detection methods have made use of advanced signal processing techniques. For example, Reed et al. [16] have used Dempster-Shafer information to classify mines for reduction of false alarms; and Dura et al. [4] have proposed a data-adaptive algorithm to eliminate the need for *a priori* training of MCM missions. Improvements to traditional Bayesian detection methods, including usage of geometric and statistical properties of objects have been proposed by Calder et al. [1]. Maussang et al. [9] [10] have applied adaptive data thresholding for object detection as well as statistical methods that do not require the presence of a shadow for mine detection, which is useful for detecting buried mines.

Recently, Ray and coworkers [5], [13], [15] have developed a pattern identification technique called Symbolic Dynamic Pattern Analysis, which compresses large data sets into pattern vectors of much lower dimension. The underlying concept is built upon the principles of multiple disciplines including *Statistical Mechanics* [11], *Symbolic Dynamics* [7], *Statistical Pattern Recognition* [3], and *Information Theory* [2]. The symbolic pattern analysis algorithm has been experimentally validated for real-time execution in diverse applications, including electronic circuits [14] and fatigue damage monitoring in polycrystalline alloys [5], and robot signature analysis [8]. This technique has been shown to be superior for pattern classification to Bayesian filtering, Neural networks and other statistical methods in terms of speed of execution, memory requirements, and robust detection in the presence of noise [14].

This paper proposes symbolic pattern analysis of sidescan sonar images for detection of underwater mines. The proposed method has been trained and validated on a set of sonar data in the form of images collected by Naval Surface Warfare Center. Section II presents data formatting and a geometric model for pattern analysis. Section III provides a

★This work has been supported in part by the U.S. Office of Naval Research under Grant Nos. N00014-07-1-0288 and N00014-08-1-380 and by the U.S. Army Research Office (ARO) under Grant No. W911NF-07-1-0376. The authors would like to acknowledge Naval Surface Warfare Center - Panama City Division, Panama City, Florida for providing the data used in this publication. Any opinions, findings and conclusions or recommendations expressed in this publication are those of the authors and do not necessarily reflect the views of the sponsoring agencies.

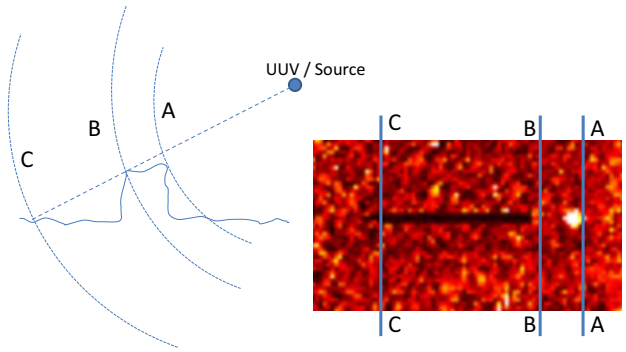

Fig. 1. Sonar wave reflections from a mine

brief review of symbolic dynamics, space partitioning methods, and construction of a Markov machine for development of the mine detection algorithm. Section IV constructs the classifier and the sliding window model to scan images. Section V shows the results of executing the pattern analysis algorithm on a test data set. Section VI concludes the paper with recommended directions for future work.

II. Data Formatting for Mine Detection

With the objective of formulating a mine detection algorithm, this section presents formatting of the sidescan sonar data sets that are structured in the form of images. Ground-truth information is available for a set of images acquired by a UUV about the location of mines. The ensemble of data sets is partitioned into a training set of 100 images and a test set of 100 images for further analysis. Parameters required for the application of symbolic dynamics, such as alphabet size are chosen based on the ground-truth statistics. A geometric model, similar to [1] has been used for feature extraction to detect and classify mines in a sonar trace. This model is used in the training set to obtain the distributions of the various regions of a mine. A sequence of tests is determined to characterize a mine according to the identified distributions.

A. Geometric modeling of mines

Based on the principles of sidescan sonar operation and properties of sound wave propagation in the oceans, a mine is characterized by three distinct regions that correspond to a bright spot, a shadow and the clutter around both bright spot and shadow.The principle of mine detection using sidescan sonars is illustrated in Fig. 1.

A mine is usually made of a denser material than other seabed objects; hence, the reflection off a mine is usually much stronger than those from its surroundings. There is also a sonar shadow due to the structure of the mine protruding off the sea bed; this shadow is a very useful indicator for distinguishing mines from the background features. Therefore, a mine usually appears as a bright object; and since the mines under consideration are placed on the seabed, there is a shadow region that exists adjacent to a mine in the direction away from the sidescan sonar receiver. There are

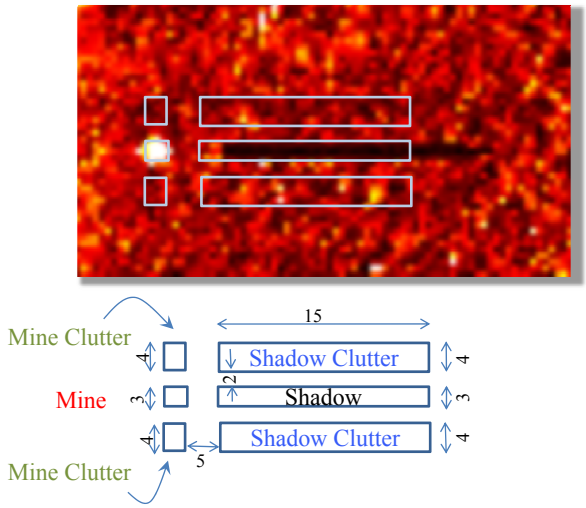

Fig. 2. Geometric model for mine detection

also clutter regions around the mine and the shadow. This clutter region around mine and its shadow is an important feature to distinguish mines from larger objects on the sea bed which also cast shadows behind them (e.g., large rocky structures on the seabed).

Therefore, the geometric model for mine detection is formulated by taking into consideration the following four distinct regions: (a)Main body of the mine, characterized by a bright spot (b)Shadow of the mine, characterized by a dark region (c)Clutter around the mine(d)Clutter around the shadow.

In general, mines are spatially isolated from each other and are accompanied by clutters. Figure 1 shows the sonar ray reflection model along with a typical mine present on the sea bed. The model for mine detection is parameterized based on the following aspects: (i) geometric properties of the expected objects, (ii) size parameters estimated from the objects present in the ground truth, and (iii) physical understanding of the relative importance of the various components of the geometric model.

Model parameterization reduces the mine detection process to comparison of various statistics generated from ground-truth analysis. The model along with its parameters is exhibited in Fig. 2 that displays the number of pixels allocated to each region in the image, where each pixel corresponds to an area of $\sim 3{\times}6\ cm^2$.

III. Symbolic Pattern Analysis

This section presents the underlying concepts and salient features of *symbolic pattern analysis* method. While the details of this method have been reported in previous publications for one dimensional time series data analysis [13], [15], this paper extends the concepts of symbolic pattern analysis for two-dimensional data (i.e., an image) analysis and presents an application for detection of undersea mines in sonar images.

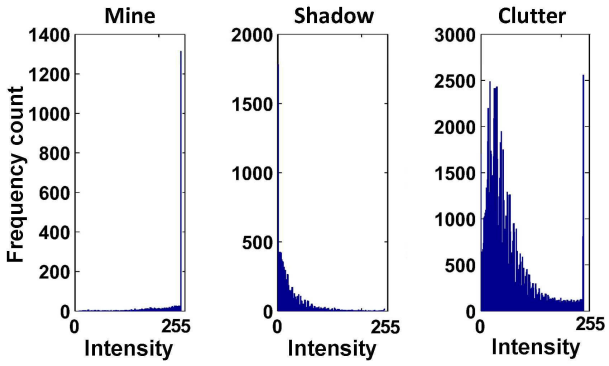

Fig. 3. Histogram of sonar wave reflections for mines, shadows and clutter. The distribution of pixel intensities in the regions of mine-clutter and shadow-clutter showed similar trends, therefore, they have been combined together in a single histogram of clutter region.

A. Construction of the Partitioning Scheme

Two important parameters need to be determined for successful partitioning of data. The first parameter is the alphabet size $|\Sigma|$ and the second is the vector of the partition segment boundaries. In this application of mine detection, the essential robust features that need to be preserved are the bright reflections from the front of an object protruding above the sea bed, and the long shadow that follows the object. Apart from this information, clutter is an important feature that has been used in the pattern analysis presented in this paper. It is observed that only three symbols are sufficient to characterize the features of interest. Figure 3 shows histograms of density functions for mine, shadow, and clutter regions. The histograms depict the number of pixels vs pixel intensity for each region. These histograms are generated from the a priori known ground-truth information about the exact location of mines from the training data set of 100 sonar images. The histograms for the three regions are clearly separated. Therefore, a distinct single symbol in the alphabet Σ is assigned to each of the three features corresponding to mine, shadow and the clutter. The information gained by increasing the alphabet size is found to be too little to offset the additional computation. A point to note from the clutter histogram in Fig. 3 is that a small neighborhood around the mine region causes more bright spots from the mine to be relegated to the clutter region.

The next important consideration is selection of segment boundaries of the partition. Traditional partitioning techniques (e.g., uniform partitioning and maximum entropy partitioning [13]) may not adequately capture the details of mine patterns; and conventional data-driven partitioning methods lead to a large alphabet size. This paper makes use of the statistical model information from the three histograms in Fig. 3. Partitioning is constructed by assigning symbol a to high intensity pixels ranging from 180 to 255 on the gray scale; similarly, symbol b is assigned to medium intensity pixels ranging from 56 to 179; and symbol c is assigned to low intensity pixels ranging from 0 to 55. As seen from Fig. 3, approximately 97% of the pixels in the mine histogram correspond to the symbol a (i.e., bright pixels); similarly, approximately 89% of the pixels in the shadow histogram correspond to the symbol c (i.e., dark pixels). A majority of the remaining (i.e., moderately dark) pixels corresponding to the symbol b belong to the clutter region. Thus, the entire image is then symbolized and represented by a two dimensional array of symbols belonging to the set $\Sigma = \{a, b, c\}$. This partitioning scheme enables robust detection of mines with a high probability of detection and a very low probability of false alarms as discussed in the results section. Further, this symbolization greatly reduces the amount of memory required for any processing. The next subsection explains the method of feature extraction using the geometric model for mine detection.

B. Feature Extraction

A finite state Markov machine is now constructed, where the set of machine states is isomorphic to the symbol alphabet Σ [15]. As there are three symbols in Σ, the dimension of the state space is also 3. Symbol a corresponds to a bright pixel state in the sonar image, while symbol c corresponds to a dark pixel state that may be a part of a shadow. Symbol b denotes a 'mid-level' pixel state.

A region $\mathcal{B}$ in the image space represents one of the three regions in the geometric model, i.e, the mine region, the shadow region, and the clutter region. The Markov assumption allows construction of the state probability vector $\mathbf{p}$ that is chosen to be the feature vector for a given bounded region $\mathcal{B}$. The elements of $\mathbf{p} \triangleq [p_a \; p_b \; p_c]^T$ are calculated by frequency counting as:

$$p_i = Prob\,(\sigma_i \in \Sigma|\mathcal{B}) \approx \frac{N(\sigma_i)}{\sum_{j\in\{a,b,c\}} N(\sigma_j)}, \; i = a, b, c \quad (1)$$

where $N(\bullet)$ is the count of $\bullet$ in $\mathcal{B}$.

The construction of the feature vector $\mathbf{p}$ follows the sliding block code [7], where sliding of the geometric model (described in Section II) along the sonar image is depicted in Fig. 4. For every pixel location (i, j), the geometric model is constructed around that pixel, such that (i, j) lies at the center point of the mine region. In this way, the feature vector is generated for each region of the geometric model. Therefore, for any pixel location (i, j) on the sonar image, the following four feature vectors (see Fig. 2) are generated.

1) $\mathrm{P}^M(i,j) = \left[p_a^M(i,j)\, p_b^M(i,j)\, p_c^M(i,j)\right]^T$ is constructed from the **mine** region.
2) $\mathrm{P}^S(i,j) = \left[p_a^S(i,j)\, p_b^S(i,j)\, p_c^S(i,j)\right]^T$ is constructed from the **shadow** region.
3) $\mathrm{P}^{MC}(i,j) = \left[p_a^{MC}(i,j)\, p_b^{MC}(i,j)\, p_c^{MC}(i,j)\right]^T$ is constructed from the **clutter** region around the **mine**.
4) $\mathrm{P}^{SC}(i,j) = \left[p_a^{SC}(i,j)\, p_b^{SC}(i,j)\, p_c^{SC}(i,j)\right]^T$ is constructed from the **clutter** region around the **shadow**.

IV. Classifier Construction

This section presents construction of a classifier for identification of mines and non-mine-like objects. Four scalar parameters, η^M, η^S, η^{MC}, η^{SC}, (that are dependent on the pixel location (i, j)) are derived from the four feature vectors at each pixel location as follows.

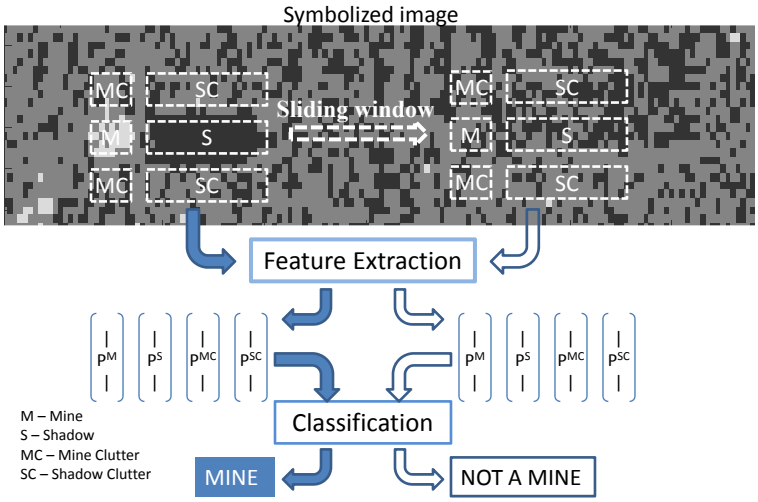

Fig. 4. Symbolic dynamics-based mine detection

$$\eta^M(i,j) \triangleq [1\,0\,0]\mathrm{P}^M(i,j) \quad (2)$$
$$\eta^S(i,j) \triangleq [0\,0\,1]\mathrm{P}^S(i,j) \quad (3)$$
$$\eta^{MC}(i,j) \triangleq [0\,1\,1]\mathrm{P}^{MC}(i,j) \quad (4)$$
$$\eta^{SC}(i,j) \triangleq [1\,1\,0]\mathrm{P}^{SC}(i,j) \quad (5)$$

Here, η^M corresponds to the fraction of bright pixels (state a) found in the mine cluster region. Typically, for a mine, η^M is expected to exceed a certain threshold. Similarly, η^S corresponds to the fraction of dark pixels (state c) in the shadow region and is expected to exceed a threshold for a mine. In the clutter region around the mine, η^{MC} represents the combined fraction of dark and 'mid-level' pixels (states c and b); therefore, η^{MC} is expected to be large around a mine implying that a mine clutter must be darker as compared to the mine. Similarly, in the clutter region around the shadow, η^{SC} represents the combined fraction of bright and 'mid-level' pixels (states a and b); therefore, η^{SC} is expected to be large around a shadow implying that a shadow clutter must be relatively less dark as compared to the shadow.

A threshold-based classification rule is formulated to identify a mine from the sonar data sets in the form of images. Given appropriately chosen scalar thresholds λ_1, λ_2, λ_3, and λ_4, the following conditions must be satisfied for a pixel (i,j) to be classified as part of a mine.

- $\eta^M(i,j) \geq \lambda_1$
- $\eta^S(i,j) \geq \lambda_2$
- $\eta^{MC}(i,j) \geq \lambda_3$ and $\eta^{SC}(i,j) \geq \lambda_4$

The above four scalar thresholds, (λ_1, λ_2, λ_3, and λ_4), are chosen based on the receiver operating characteristics (ROC) [12] to yield different choices of probability of detection (P_D) and false alarm rate (FAR), which are defined in terms of percentage of correctly detected mines and the number of mines falsely detected per image, respectively. (Note: The size of an image is 1000×512 pixels.)

A. Receiver Operating Characteristics

A sliding window method is used to implement the geometric model in Section II and the classifier described above.

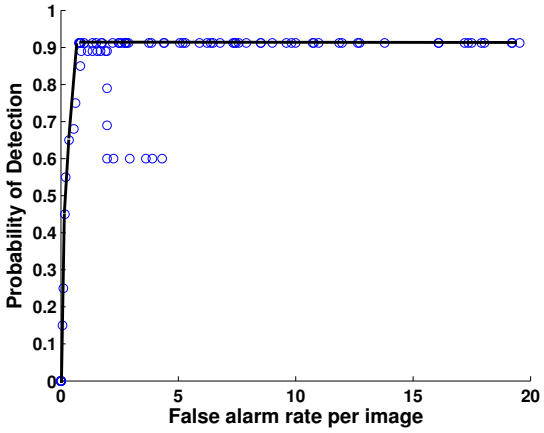

Fig. 5. Receiver Operating Characteristics for Symbolic Dynamics based detection

For each pixel in the image, a model is constructed, as shown in Fig. 4. Assuming that the pixel under consideration is at the center of the mine region, the four feature vectors $\mathrm{P}^M, \mathrm{P}^S, \mathrm{P}^{MC}$ and P^{SC} are generated. Then, the classification scheme is applied and a binary decision is made to determine whether the pixel location belongs to a potential mine. A binary number of 1 or 0 is assigned to each pixel of the image based on the classification as a mine or non-mine-like object, respectively.

To construct the receiver operating characteristics (ROC), a test data set consisting of 100 images is considered. These images consist of various textured backgrounds, with different types of sea-bed objects and vehicle-induced image artifacts. The images are in the range of 0 to 255 on the gray scale. Each of the four thresholds (i.e., λ_1, λ_2, λ_3 and λ_4) are varied from 0 to 1 in steps of 0.1 and the pattern analysis algorithm is executed over the entire set of test data. The number of false alarms, and the number of correct detections are counted in each threshold parameter combination. The ROC plot is constructed by joining the outermost points on

the plot of probability of detection (P_D) versus false alarm rate (FAR) per image as shown in Fig. 5. For subsequent analysis, the chosen thresholds (λ_1 = 0.8, λ_2 = 0,7, λ_3 = 0.4 and λ_4 = 0.4) gives a probability of detection of 92% and 1.5 false alarms per image (or $900m^2$)

V. Results and Discussion

This section presents the results generated upon execution of the pattern analysis algorithm on one hundred images from the test data set that is different from the training data set used to generate the partition. As an example, four of these images are shown in Fig. 6, where the results of detection are shown in the right hand side of each plate from (a) to (d).

Four representative images are shown in Fig. 6, each showing different levels of background noise, and sea-bed clutter. A representative set of threshold values is chosen to yield a high detection probability with an acceptable false alarm rate. An appropriate operating point is chosen on the ROC curve based on the premise that a missed detection costs much higher than a false alarm. Tests show that the algorithm is capable of detecting mines in a high concentration of sea-bed clutter, including mines buried under vehicular artifacts. The algorithm has been executed on the entire set of test data with the same values of representative thresholds; Table I lists false alarms and successful detections. With alternative choices of operating points on the ROC curves, the mine detection probability can be increased at the expense of increased false alarm rate as a trade-off between Type I and Type II errors.

VI. Summary, Conclusions and future work

This paper presents a data-driven symbolic dynamic based method of mine detection for the purpose of mine counter measures. The use of a template based method allows for the introduction of prior knowledge. The use of Symbolic Dynamics improves noise robustness, and enables the real time implementation of the whole algorithm.

On a sonar data set in the form of images, a template was constructed and symbolic dynamic parameters were determined. A ground truth was provided, which enabled the construction of alphabet and partition segment locations. The algorithm was then tested on a different test set of images on which the probability of detection was $\sim 91.5\%$ with an average of ~ 1.25 false alarms in a 1024×512 pixel area (approximately 2 square kilometers). Several test images were shown, with varying degrees of noise and sea-bed clutter, and the algorithm was shown to function well in all conditions.

A key aspect to the performance of the proposed mine detection method is the construction of the geometric model. Different regions in the model are carefully chosen to match the sizes of the objects to be detected. A conservative estimate is made on all counts so that the smallest possible objects can be detected. However, even with these conservative estimates that enable a high detection probability, a relatively low rate of false alarms is still unavoidable.

TABLE I

Results of running Symbolic Dynamic based and a log-likelihood based pattern analysis on a test data set

Description	Value
Number of Images Analyzed	100
Number of Mines (Ground Truth)	100
Probability of Detection (P_D)	$\sim$91.5%
False alarm rate (FAR) per image	$\sim$1.5

Tests based on real-life data show that a high percentage of mines is detected with a low false alarm rate. However, a shortcoming of the proposed method is its inability to detect objects that are smaller than the smallest object in the training set. This is evident from the ROC curve that the probability of detection can never reach 1 because some mines do not fit the nature of the model template.

The major advantages of the proposed pattern analysis algorithm for underwater mine detection are delineated below.

1) Performance of the pattern analysis algorithm is robust with respect to locations of the segment boundaries of the partition. The important aspect is that the partitions must correspond to the three characteristic features, namely, mine, shadow and clutter.
2) The algorithm is computationally efficient in terms of execution time and memory requirements as a consequence of a small alphabet and a small number of states in the Markov machine of the algorithm. As such the entire algorithm can be programmed and powered on a small microprocessor on-board a UUV.
3) In contrast to traditional Bayesian methods such as the likelihood-ratio-test, the symbolic pattern analysis does not require *a priori* knowledge of probability distribution for characterizing mines and non-mine-like objects. Specifically, the proposed algorithm is robust even if the unknown distributions are multi-modal.

Further theoretical and experimental research is necessary before the proposed algorithm can be considered for implementation in the ocean environment. While there are many such issues, the following topics are under active research.

- Development of advanced measurement techniques and algorithms to distinguish between mines and mine-like objects that might have been falsely identified as mines;
- Testing under real-life scenarios that include varying bathymetric properties, various ocean depths and different sea states;
- Investigation of measurement test techniques in areas of higher water turbulence, which are susceptible to false alarms;
- Testing of the algorithm performance for simultaneous enhancement of successful detection and reduction of false alarms through additional measurements such as multiple scanning from from different angles;
- Enhancement of algorithm performance through usage of flexible templates (e.g., varying shadow lengths).

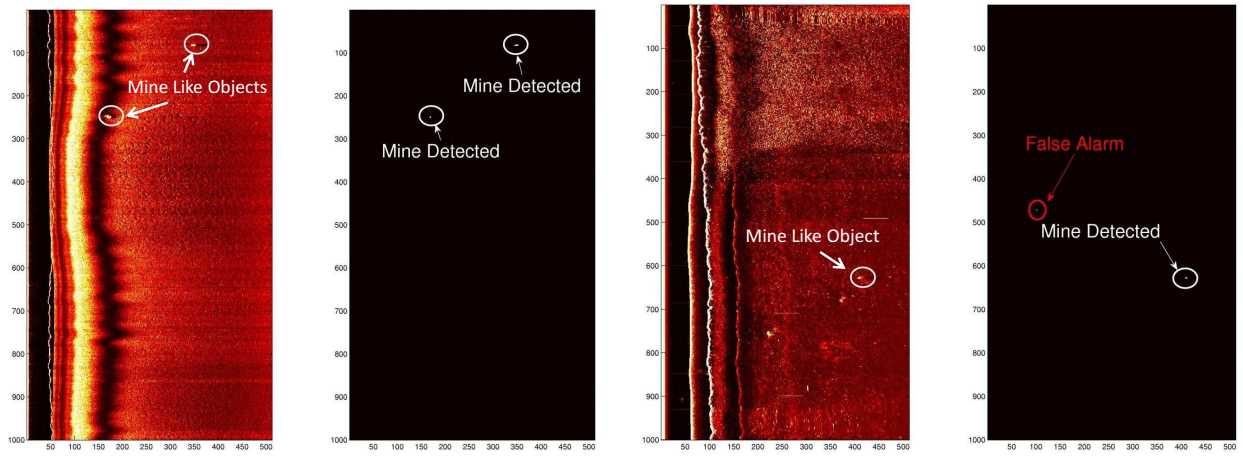

(a) Symbolic Analysis for a clean image

(b) Symbolic Analysis for a slightly noisy image

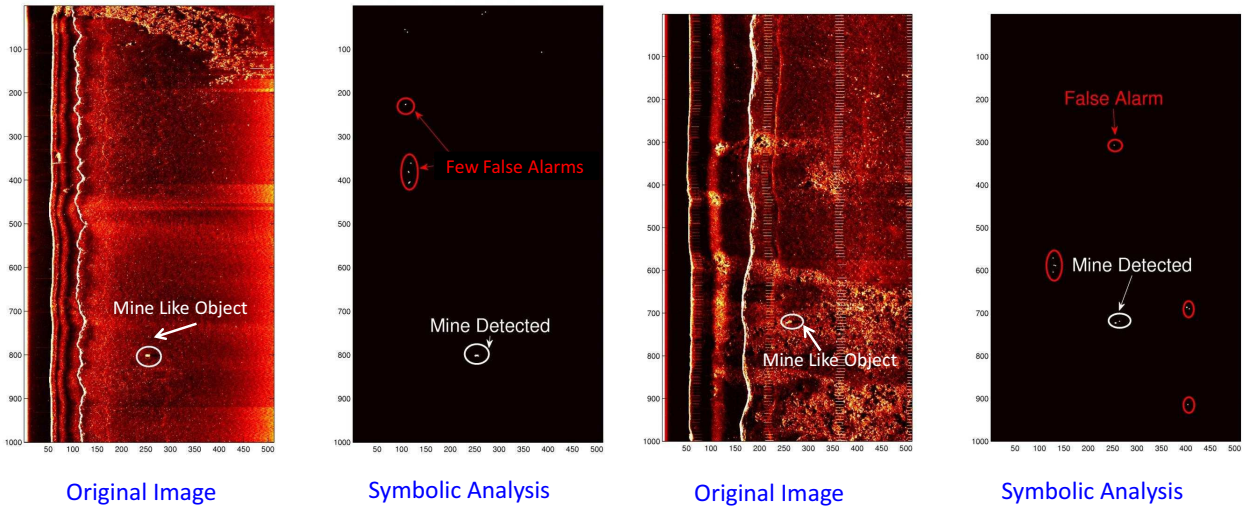

(c) Symbolic Analysis for a noisy image

(d) Symbolic Analysis for a very noisy image

Fig. 6. Representative images from test data set

REFERENCES

[1] B.R. Calder, L.M. Linnett, and D.R. Carmichael, *Bayesian approach to object detection in sidescan sonar*, IEE Proceedings -Vision, Image and Signal Processing **145** (1998), no. 3, 221–228.

[2] T. M. Cover and J. A. Thomas, *Elements of information theory*, first ed., Wiley Interscience, New York, 1991.

[3] R. O. Duda, P. E. Hart, and D. G. Stork, *Pattern classification*, 2nd edition ed., Wiley Interscience, New York, NY, 2001.

[4] E. Dura, Y. Zhang, X. Liao, G.J. Dobeck, and L. Carin, *Active learning for detection of mine-like objects in side-scan sonar imagery*, IEEE Journal of Oceanic Engineering **30** (2003), no. 2, 360–371.

[5] S. Gupta, A. Ray, and E. Keller, *Fatigue damage monitoring by ultrasonic measurements: A symbolic time series analysis approach*, International Journal of Fatigue **29** (2007), no. 6, 1100–1114.

[6] D. Li, K.D. Wong, Y.H. Hu, and A.M. Sayeed, *Detection, classification, and tracking of targets*, IEEE Signal Processing Magazine (2002), 17–29.

[7] D. Lind and M. Marcus, *An introduction to symbolic dynamics and coding*, Cambridge University Press, 1995.

[8] G. Mallapragada, I. Chattopadhyay, and A. Ray, *Automated behavior recognition in mobile robots using symbolic dynamic filtering*, Journal of Systems and Control Engineering (2008).

[9] F. Maussang, J. Chanussot, A. Hetet, and M. Amate, *Meanstandard deviation representation of sonar images for echo detection: Application to sas images*, Oceanic Engineering, IEEE Journal of **32** (2007), no. 4, 956–970.

[10] F. Maussang, M. Rombaut, J. Chanussot, A. Htet, and M. Amate, *Fusion of local statistical parameters for buried underwater mine detection in sonar imaging*, EURASIP Journal on Advances in Signal Processing (2008), no. 876092, 19.

[11] R.K. Pathria, *Statistical mechanics*, 2nd ed., Butterworth-Heinemann, Oxford, UK, 1996.

[12] V. Poor, *An introduction to signal detection and estimation*, 2nd ed., Springer-Verlag, New York, NY, USA, 1988.

[13] V. Rajagopalan and A.Ray, *Symbolic time series analysis via wavelet-based partitioning*, Signal Processing **86** (2006), no. 11, 3309–3320.

[14] C. Rao, A. Ray, S. Sarkar, and M. Yasar, *Review and comparative evaluation of symbolic dynamic filtering for detection of anomaly patterns*, Signal, Image, and Video Processing (2008), DOI 10.1007/s11760-008-0061-8.

[15] A. Ray, *Symbolic dynamic analysis of complex systems for anomaly detection*, Signal Processing **84** (2004), no. 7, 1115–1130.

[16] S. Reed, Y. Petillot, and J. Bell, *Automated approach to classification of mine-like objects in sidescan sonar using highlights and shadow information*, IEE Proc.-Radar Sonar Navig. **151** (2004), no. 1, 90–105.